Bull. Nov. Comp. Center, Math. Model. in Geoph., 18 (2015), 35–47

Trans-boundary realization of the nested-grid algorithm for trans-pacific and regional tsunami modeling

An.G. Marchuk, K. Hayashi, A.P. Vazhenin

Abstract. The grid-switching algorithm for the tsunami propagation computation from the initial source to the coastline that uses scale switching has been developed. Computations are carried out on a sequence of grids with various resolutions where one is embedded into another. Tsunami wave parameters are transferred from a larger domain to the embedded smaller one by means of the boundary conditions. Using the method proposed, the numerical simulation of tsunami generated by a model ellipsoidal source located in the middle of the Pacific was carried out.

Keywords: tsunami propagation modeling, computational grid, boundary conditions, time step.

1. Introduction

Tsunami sources are usually located in deep-water areas. So, if we want to estimate tsunami parameters near the coastline, the computational domain must include both a deep and a shallow-water areas. A standard stability condition for numerical algorithms used for the modeling requires the wave advancement per one time step be less than a spatial grid-step. In this case, we should use a small enough time step (for the computation stability in deep-water areas of the domain), which makes computations on a shallow shelf with an unreasonably small time step be time-consuming. There are a number of algorithms and models developed for the tsunami risk mitigation. The most known and in general use are TUNAMI [1] and MOST (Method of Splitting Tsunami) [2–4]. These algorithms cover the phases of generation, propagation of tsunami from the deep ocean to the coastal areas. However, the quality of the warning systems is far from being efficient to provide the population security. Now it is necessary to develop original algorithms for the real time data processing and their adaptation in order to use the whole computational power of modern hardware. Modern reliable and fast algorithms will contribute to the task of human protection in the shoreline areas. The only way to protect people living on the shoreline from catastrophic tsunami waves is to make an accurate estimation of expected tsunami wave parameters such as height near the shore, wave arrival times, etc. The numerical modeling of tsunami wave propagation takes much time and should be accelerated the sooner the better. Such an acceleration can be done with the help of hardware architectures or developing more efficient algorithms. The MOST software is used to numerically simulate three processes of the tsunami evolution: estimation of a residual displacement area resulting from an earthquake and tsunami generation, trans-oceanic propagation through deep-water zones, and contact with land (run-up and inundation). The given research is concerned with the wave propagation stage.

The long wave propagation in the ocean is governed by the so-called shallow-water differential equations:

$$\begin{aligned} H_t + (uH)_x + (vH)_y &= 0, \\ u_t + uu_x + vu_y + gH_x &= gD_x, \\ v_t + uv_x + vv_y + gH_y &= gD_y, \end{aligned} \tag{1}$$

where $H(x, y, t) = h(x, y, t) + D(x, y, t)$, h is the water surface vertical displacement, D is depth, $u(x, y, t)$ and $v(x, y, t)$ are velocity components along the axes x and y, and g is acceleration of gravity. The initial conditions: still water at all grid points except a tsunami source where a surface displacement is not equal to zero. From the shallow-water equations it follows that the tsunami propagation velocity does not depend on its length and is expressed by the so-called Lagrange formula [2]

$$c = \sqrt{g(D + \eta)}. \tag{2}$$

This formula plays the key role for the long-wave (tsunami) kinematics. From the shallow-water equations the ratio between the running wave height and the water flow velocity can be derived. The horizontal flow velocity depends on the wave amplitude and water depth

$$u = \eta\sqrt{\frac{g}{D}}\,. \tag{3}$$

These relations between tsunami wave parameters are used in the algorithm proposed.

The numerical algorithm is based on splitting the difference scheme that approximates equations (1) by spatial directions. A finite difference algorithm based on the splitting method has been developed in [2]. To solve the shallow wave equations, the splitting method reduces the numerical solution with two spatial variables to the solution of two one-dimensional equations. It makes possible to use effective finite difference schemes developed for one-dimensional problems. Moreover, this method permits one to set boundary conditions for a finite difference boundary value problem using a characteristic line method. The criterion of stability for the MOST algorithm can be written down as

$$\Delta t \le \frac{\Delta x}{\sqrt{gH}}. \tag{4}$$

Here Δt and Δx are the time and the grid steps, respectively. This condition requires setting a smaller time step if a computational domain contains deep-water areas. For example, if a deep-water trench with a depth of 9,000 m is included into the area with 1,000 m resolution computational grid, then we must use a 3-second (or less) time step for the stability of computation. At one time step, a tsunami wave must advance a distance less than one spatial grid step. In the case of tsunami occurrence, a deep-water detector can give the passing tsunami wave parameters 15–20 minutes after the main shock of a tsunamigenic earthquake. Then a few minutes are necessary to obtain the first estimates of the tsunami source parameters and its center, in particular, the location of the center (the locality of a maximum vertical displacement of the water surface) and a value of a maximum vertical elevation. This information allows us to begin the numerical calculation of a direct problem of tsunami propagation from the source, actually, to the coastline (up to depths of 5–10 m). However, for obtaining results of the tsunami propagation, be more reliable (distribution of tsunami wave heights in a shelf zone), rather a small step of a computational grid (about tens meters) is necessary. If we simulate the tsunami propagation in the whole area including both a source zone and sites of the coast, we are interested in, using this small spatial grid step, then because of the stability condition we will be compelled to carry out calculation with a small time step. This will bring about a significant increase in the time of numerical calculation that is inadmissible in real-time calculations. Therefore it is necessary to carry out such calculations with the use of the computational grids whose spatial step decreases when approaching the coast.

A standard MOST software package uses as an initial water surface elevation that is equal to the ocean bottom displacement obtained as a result of numerical modeling of the elastic-plastic problem with seismic source with specified parameters. In this case, it is not easy to set the initial water surface displacement with a specified amplitude at the desired locality. However, sometimes it is needed to study the ratio between the initial wave height and wave parameters near the coast. In this case it is necessary to carry out a number of numerical experiments with specified initial parameters. For this purpose two algorithms can be implemented into the MOST software package. The first subroutine defines the initial water surface displacement having the ellipsoidal shape. Inside this ellipse, the surface elevation is expressed by the formula

$$H(i,j) = \big(1 + \cos(\pi \arg(i,j))\big) H_0, \tag{5}$$

where H_0 is the half of the water surface displacement at the central point $(i_0,\, j_0)$ of the ellipse. The parameter $\arg(i,j)$ gives the ratio between the distance to the ellipse center and the distance to the ellipse border in this direction

$$\arg(i,j) = \left(\frac{(i-i_0)\cos\beta + (j-j_0)\sin\beta}{r_1}\right)^2 + \left(\frac{(j-j_0)\cos\beta - (i-i_0)\sin\beta}{r_2}\right)^2.$$

Here r_1, r_2 are the ellipse axis lengths and β is the long axis azimuth. Figure 1 shows the shape of the 2 meters height ellipsoidal source with the axes ratio equal to 2 and the water height distribution along the ellipse axis.

Thus, this subroutine gives the possibility of the numerical simulation of the tsunami waves generated by such a kind of sources with a specified location and an initial height. Another way to generate a wave with given parameters (an amplitude and a wavelength or a period) is to use boundary conditions. For example, let at the initial instant of time in the whole computational domain the water surface elevation and flow velocity components be equal to zero. Then at all the grid points along one boundary (for example, vertical) the following free boundary conditions are fulfilled during a limited time period:

$$\eta = \frac{\eta_0}{2}\left(1 - \cos\frac{2\pi t}{T}\right), \quad u = \eta\sqrt{\frac{g}{D}}, \tag{6}$$

where η_0 is a wave height and T is its period, g is the gravity acceleration, D is the depth. As a result, the flat tsunami wave having the amplitude η_0 and the period T will propagate from this vertical boundary inside the computational domain.

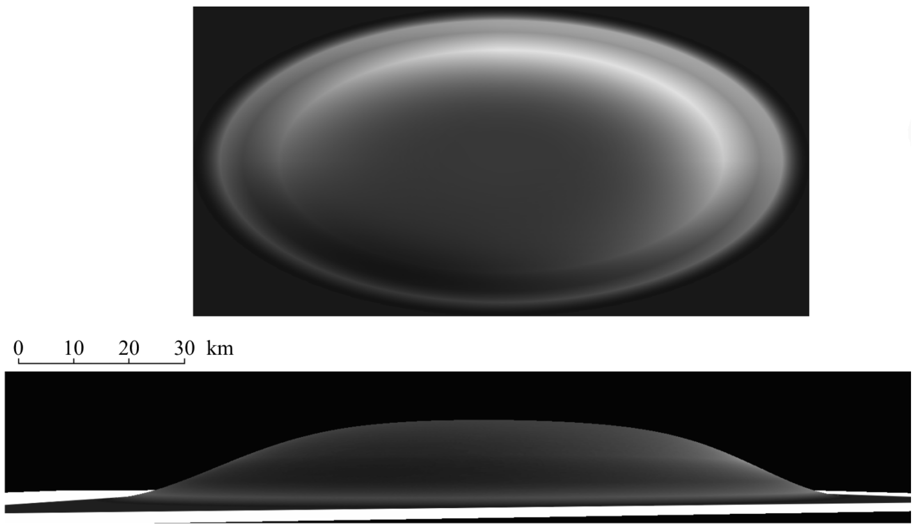

Figure 1. The shape and cross-section of a model ellipsoidal tsunami source

The multi-grid computations of the tsunami wave propagation. We propose the algorithm, which consists in a consecutive calculation of the tsunami wave propagation in several computational domains, where each subsequent computational area is a subarea to the previous one, but with a smaller spatial step. And initially in these subareas there is no tsunami source (the initial vertical water surface displacement). Information on parameters of a wave is transferred to each subsequent subarea through boundary conditions, thus these data are interpolated along the boundary on a smaller computational grid. Digital bathymetry sets were taken or developed using different sources. The first stage of the numerical simulation uses the whole-Pacific gridded bathymetry developed by Smith and Sandwell [5], which is now used by the NOAA for the trans-pacific tsunami modeling. The geographical coverage of this computational domain are shown in Figure 2.

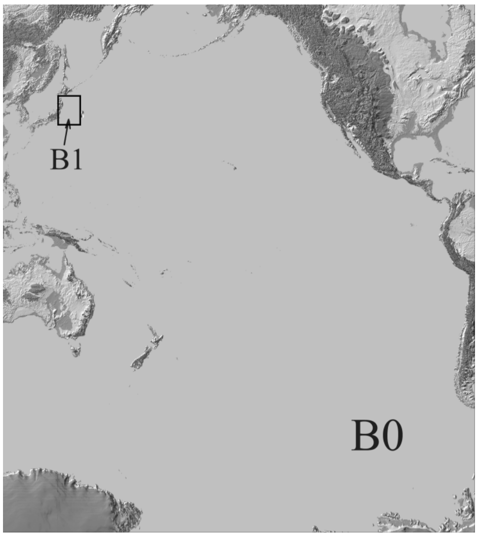

Figure 2. The coverage of the whole Pacific computational domain (B0 area)

Resolution of this digital bathymetry is varying from 4 arc minutes (about 8,000 m) at the equator to 2 arc minutes (approx. 4,000 m) closer to the polar areas. The geographic coverage of these data (area B0) is from 120° E to 68° W and from 73.96° S up to 62° N.

For further stages of the modeling, the area of the Pacific Ocean adjacent to the northwest of the island of Honshu (Japan) is chosen. The gridded digital bathymetry for the numerical modeling was developed using 500 m resolution bathymetry around Japan [6] (http://jdoss1.jodc.go.jp/cgi-bin/1997/depth500_file) by recalculating the depth to the geographical projection grid and 1 arc sec ASTER Global digital elevation model [7] (http://www.gdem.aster.ersdac.or.jp/search.jsp).

The size of a computational rectangular grid, in which knots preset values of a depth was taken as 1,610 × 1,610 knots. The length of a spatial step in both directions is equal to 0.0049688 geographical degrees that is about 550 meters in the South-North direction and about 440 m in the West-East direction. The bottom topography of this computational domain B1 is shown in Figure 3.

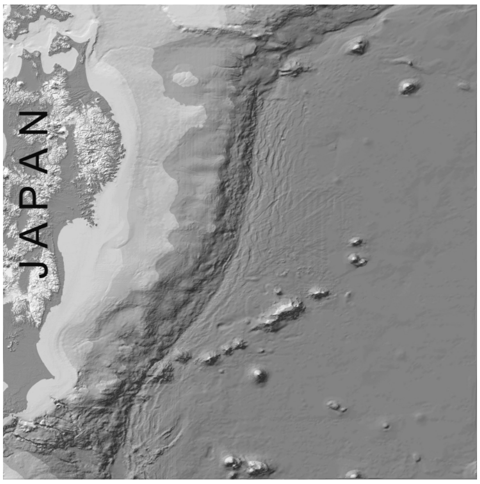

Figure 3. Visualization of the 1,610 × 1,610 gridded bottom relief around the NE coast of the Honshu island. The mesh size is 0.00496 × 0.00496 arc degrees (442 × 554 m)

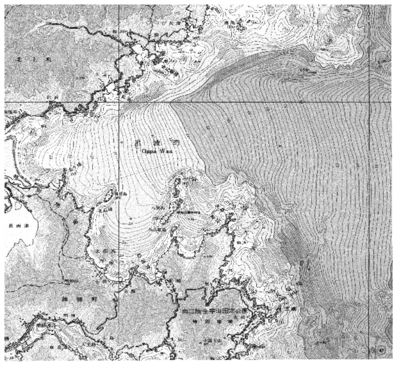

Figure 4. The scan of the bathymetric chart that was used for developing a gridded bathymetry (scale factor 1 : 50,000)

The location of B1 computational domain inside B0 area is shown in Figure 2. The B1 grid covers the geographic area from 140 to 147.9944° E and from 34.00 up to 41.9948° N. At the third stage of the numerical experiment, the 2,797 × 3,197 knots computational grid (B2), which covers the part of the Tohoku shelf area, was used. These data were developed with a linear interpolation from a segment of the B1 computational area. B2 grid covers the area from 140.745 to 142.48° E and from 37.53 up to 39.51° N. The grid resolution of the B2 area was taken 8 times less than in the B1 computational area and being equal to 0.0006211 arc degrees. At the final stage of the computational experiment, the tsunami wave entering the Sanriku coast harbors was studied. The gridded bathymetry of this small area was developed using a detailed (scale 1 : 50,000) raster bathymetric chart of the Oppa and the neighboring harbors (Figure 4).

Using the Global Mapper software the isolines of a depth in the bottom part of Figure 4 were digitized. Then the 1 arc sec resolution ASTER GDEM digital relief [7] was added, and with the help of the Global Mapper software these data were interpolated into the gridded digital bottom relief (Figure 5).

As a result, the 2148 × 1074 knots gridded bathymetry for the Oppa and the neighboring harbors was created (B3 computational domain). The length of a grid step is equal to 0.000155275 arc deg (approximately 17 m). These data cover the geographical area from 141.41659 to 141.75° E and from 38.5 up to 38.6666° N. The spatial step of the grid here is 4 times smaller

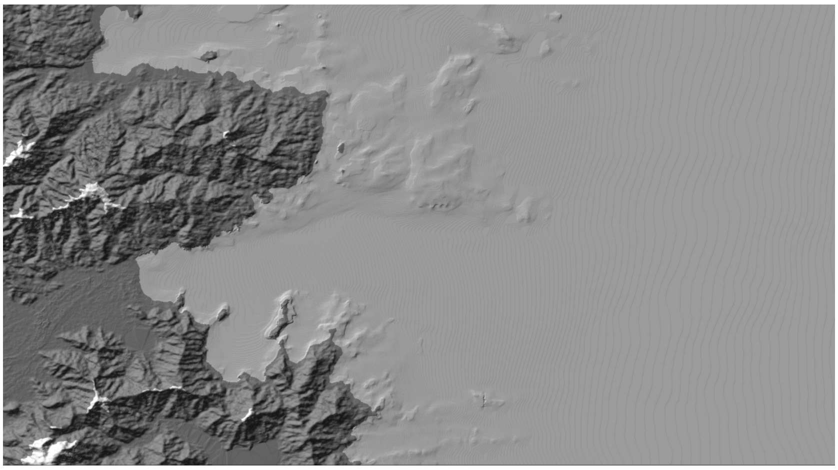

Figure 5. Visualization of the Oppa harbor bottom topography

than in B2 computational area. The location of B2 and B3 computational domains inside the B1 area is shown in Figure 6.

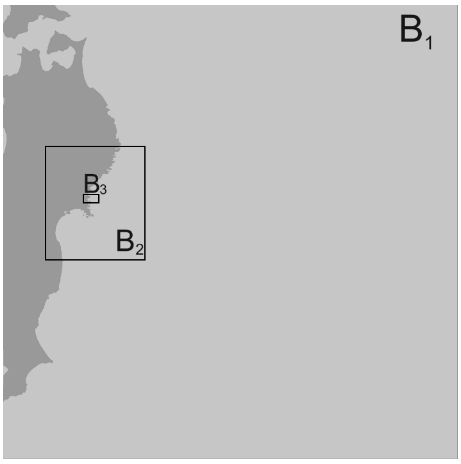

Figure 6. Location of B2 and B3 computational domains inside B1 area

The summary of these four computational grids is as follows:

B0 is the gridded 2581 × 2879 knots computational area with aprox. 4 arc-minute resolution (about 5,000 m). The time step for computations is equal to 4 s.

B1 is the gridded 1610 × 1610 knots computational area with 0.00496 arc-degree resolution (about 560 m). The time step for computations is equal to 0.5 s.

B2 is the gridded 2797 × 3197 knots computational area with 0.000621 arc-degree resolution (about 70 m). The time step for computations is equal to 0.5 s.

B3 is the gridded 2148×1074 knots computational area with 0.000155 arc-degree resolution (about 17 m). The time step for computations is equal to 0.25 s.

At the first stage of the simulation, the process of tsunami generation by the ellipsoidal initial ocean surface displacement (see Figure 1) and the following wave propagation in a deep ocean was carried out. The model tsunami source of the ellipsoidal shape is located not far from the right border of the computational subarea B1. The axis length taken was 210 km

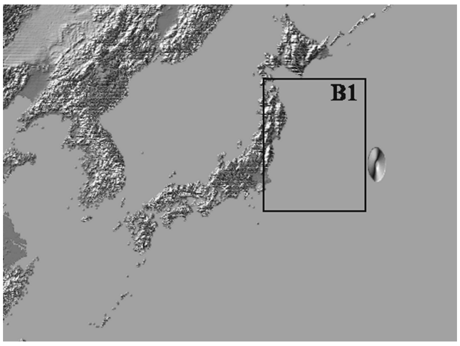

Figure 7

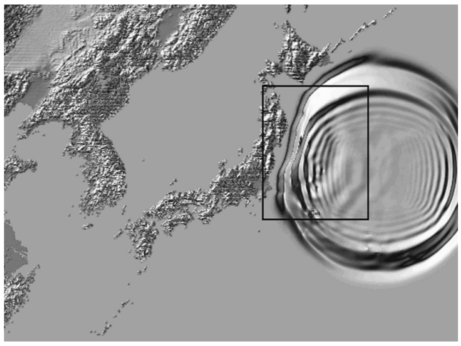

Figure 8

in the vertical direction and 80 km in the horizontal one (Figure 7). The level elevation value at the source center was equal to 200 cm. The distance off B1 computational area boundary was chosen sufficiently small in order not to wait too long for the tsunami arrival to this boundary. Figure 7 presents a zoomed segment of B0 area with the initial tsunami source.

In Figures 7, 8, the ocean surface at several instants of time is visualized. The black rectangle shows the B1 area boundary location.

At the first stage of the numerical experiment, the wave propagation in the "large" computational domain B0 almost up to the coast of Japan was simulated. The time step for this computation was equal to 4 s. In the whole process of computation, the wave parameters (amplitude, horizontal velocity components and geographical coordinates) at all the grid points along B1-area boundaries were output into a file. The data output starts from the very first time step and continues at every time step. Data recording can be stopped when a tsunami wave has passed the right boundary of the subarea B1 (at least the whole wave period). The gridded bathymetries of computational areas B0 and B1 are not well correlated. This means that there are almost no grid points having same geographic location. As was already noticed the grid-step length in these two areas significantly differs (about 5,000 m against approximately 560 m).

Using the linear interpolation, the tsunami wave parameters at B1 boundary grid-points being calculated from B0 area grid points which are most closely situated to the boundary of B1. If time steps are different, wave parameters must also be interpolated with respect to time. Thus, after recalculating the flow parameters along B1 boundaries, the second stage of the numerical experiment can be started. In this computational area, the boundary value problem is solved. The ocean surface elevation at several instants of time is visualized in Figures 9, 10.

In the course of computations in the area B1, the flow parameters values along the boundaries are to be read at every time step and the flow

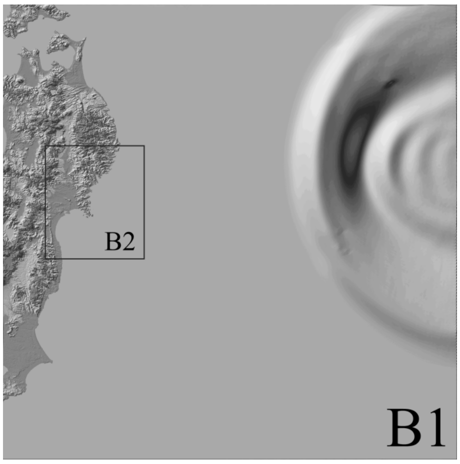

Figure 9

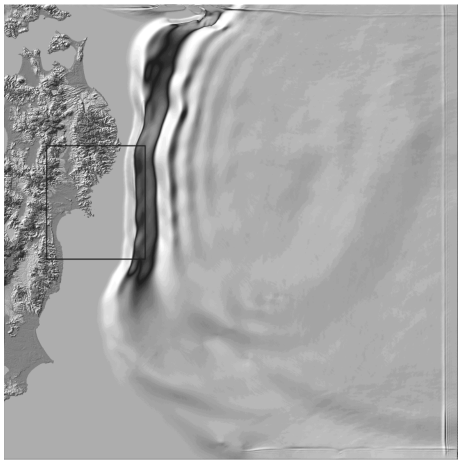

Figure 10

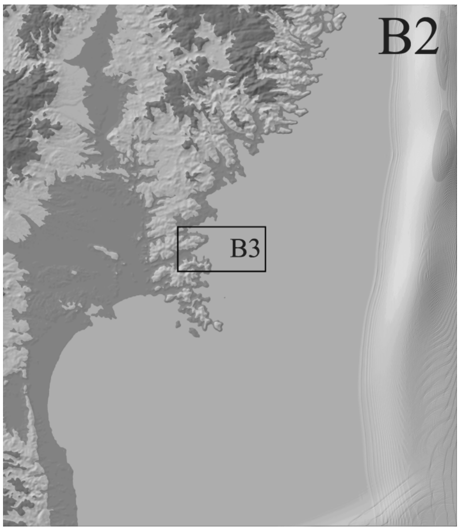

Figure 11

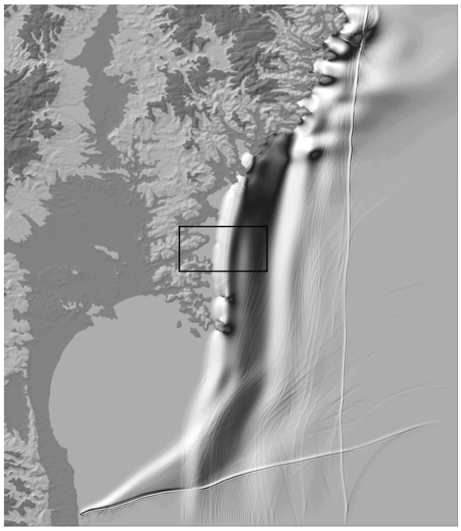

Figure 12

parameters along B2 subarea boundaries (see Figure 6) being a result of the numerical computation are also to be saved in a new file. After finishing the numerical simulation of the tsunami propagation in B1 computational domain, the boundary data from this file are to be recalculated to a more detailed grid with the help of linear interpolation. Then the third stage of the numerical experiment is ready to be started. As was performed at the previous stages, the boundary value problem in B2 area is being numerically solved. The results of this simulation are presented in Figures 11, 12.

As was done at the previous stage of this numerical experiment, a new data file containing the wave parameters along the boundaries of B3 computation subarea was created. Then, as usual, these data are to be recalculated to a more detailed grid that will be used in B3 computational domain. Due to the fact that the fourth stage of the numerical experiment is declared as the last one, no boundary data are to be saved in computations in the B3 area. The results of the numerical modeling near the Sanriku coast and inside the Oppa harbor are presented in Figures 13, 14.

Thus, a sequence of actions which we call "the trans-boundary realization of the nested-grid algorithm for the numerical modeling of tsunami propagation" is described and shown on an example. Using this algorithm, the influence of a wavelength and resolution of computational grids on the tsunami height near the coastline was studied. The process of tsunami wave propagation generated by two model ellipsoidal tsunami sources having a different

Figure 13

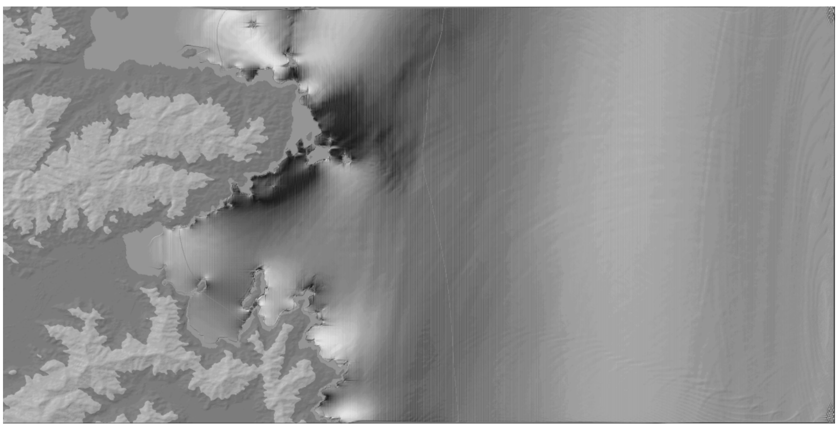

Figure 14

size was numerically computed. Each case was simulated using a “rough” grid (270 m). Then computations use grid switching from a “rough” to an “intermediate” (approx. 70 m) grid. And, finally, the numerical experiment was carried on with the help of the 3-stage multi-grid algorithm (B1, B2, and B3 domains). These numerical experiments were carried out for the model ellipsoidal sources that generate a tsunami having period 200 and 500 s (“small” and “large” sources). Let us consider the first case (a shorter wave). Figure 15 presents the water surface inside the Oppa harbor as a result of the numerical modeling using B1 computational grid. Another picture (Figure 16) shows the results obtained in the same geographic area at the same instant of time using 2-stage grid switching (from B1 to B2 grids). Figure 17 shows a zoomed segment of Figure 16. Figure 18 presents the results of numerical computations of the same problem (propagation of the tsunami generated by a “small” ellipsoidal source using 3-stage grid switching.

The comparison of tsunami parameters near the shore (in the harbors) shows a much better quality of the tsunami simulation using the grid-switching computations (see Figure 16) as compared to the results of modeling in the whole computational domain B1 (see Figure 15). Also, a significant difference between the two-grid and the three-grid numerical experiments can be easily seen. It is clear that on the rough computational grid, the wave in harbors is longer. Its amplitude is lower and it is much more reflected off the near-costal bottom slope (see Figures 17 and 18). A similar trend is seen when the “long” wave propagates through B1–B2–B3 computational areas. Here we give the summary of the detected leading wave height inside the Oppa harbor (Figure 19).

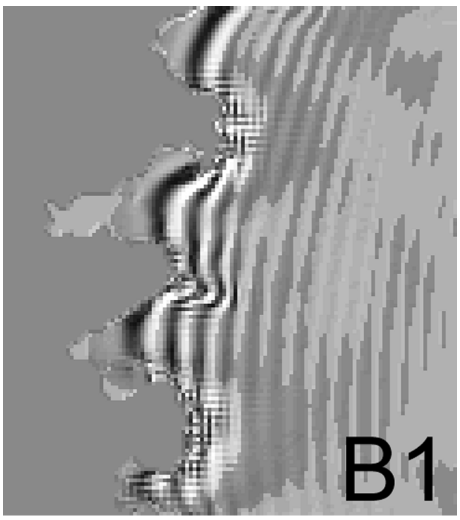

Figure 15

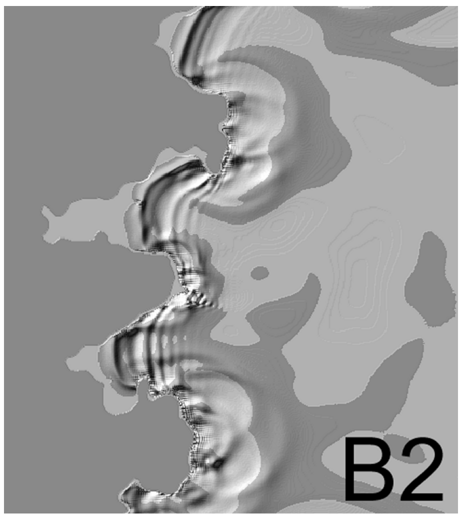

Figure 16

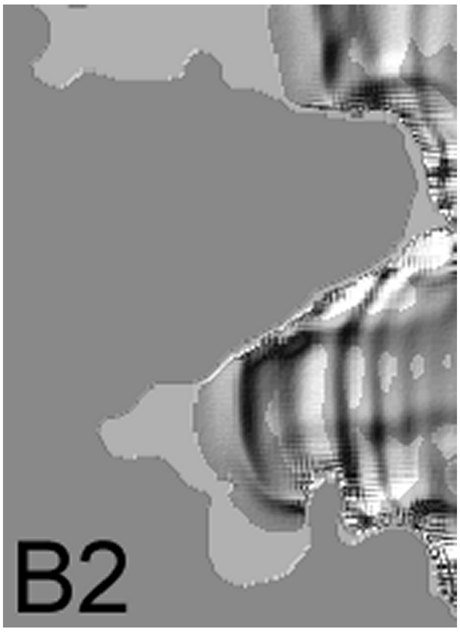

Figure 17

Figure 18

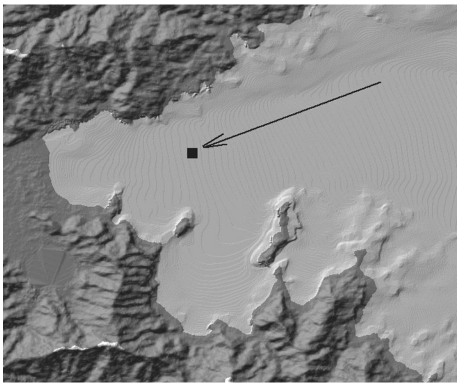

Wave period, s	Leading wave height, m		
	B1 grid	B2 grid	B3 grid
200	0.5	1.5	1.9
500	0.9	1.6	1.9

Figure 19. Location of the data output inside the Oppa harbor and leading wave height summary

These data show that for a shorter tsunami wave the effect of using the multi-grid algorithm is greater than that for long tsunami waves (a period greater than 8 minutes).

Conclusion

Computational grids must have different spatial resolutions when modeling tsunami propagation in the deep ocean and on the shallow shelf.

Tsunami wave parameters can be transmitted from a larger domain to the embedded smaller one by means of boundary conditions.

The method proposed effectively works in the case of poor correlated gridded bathymetries with different resolutions.

The method was implemented into the standard MOST software and tested on the tsunami propagation modeling in the areas with a real bathymetry around Japan.

References

[1] Shuto N., Imamura F., Yalciner A.C., Ozyurt G. TUNAMI N2: Tsunami Modeling Manual. — http://tunamin2.ce.metu.edu.tr.

[2] Titov V.V. Numerical modeling of tsunami propagation by using variable grid / Computing Center Siberian Division USSR Academy of Sciences, Novosibirsk, USSR // Proc. of the IUGG/IOC International Tsunami Symposium. — 1989. — P. 46–51.

[3] Titov V.V., Synolakis C.E. Numerical modeling of tidal wave runup // J. Waterway, Port, Coastal and Ocean Engineering. — 1998. — Vol. 124. — P. 157–171.

[4] Titov V.V. Method for numerical modeling of tsunami taking into account the wave transformation in shallow water. — Novosibirsk, 1988. — (Preprint / Computing Center SD USSR Academy of Sciences; 771) (In Russian).

[5] Smith W.H.F., Sandwell D. Global seafloor topography from satellite altimetry and ship depth soundings // Science. — 1997. — Vol. 277. — P. 1956–1962.

[6] http://jdoss1.jodc.go.jp/cgi-bin/1997/depth500.

[7] http://www.gdem.aster.ersdac.or.jp/search.jsp.